European Conference on Computational Fluid Dynamics
ECCOMAS CFD 2006
P. Wesseling, E. Oñate and J. Périaux (Eds)

AN INVESTIGATION OF THE PERFORMANCE OF A HIGH-ORDER ACCURATE NAVIER– STOKES CODE

Gunilla Efraimsson*, **Jing Gong**†, **Magnus Svärd**** **and Jan Nordström**† ‡

*Dept of Aeronautical and Vehicle Engineering, KTH
SE–100 44 Stockholm, Sweden
e-mail: gef@kth.se
†Uppsala University,
Dept of Information Technology
e-mail: jing.gong@it.uu.se
P.O. Box 337, SE–751 04 Uppsala, Sweden
*Stanford University, Center for Turbulence Research
Stanford CA 94395–3035, USA
e-mail: svard@stanford.edu
‡Swedish Defence Research Agency, FOI
Division of Systems Technology
SE–164 90 Stockholm, Sweden
e-mail: jan.nordstrom@foi.se

Key words: High-Order accurate scheme, Navier-Stokes Equations, Summation by Parts, Cavity flow

Abstract. *A high–order accurate multi–block parallel Navier-Stokes code is evaluated and tested by considering the flow over a cavity in two space dimensions. Both shear layer mode and wake mode is studied. The efficieny, robustness and flexibility of the code is demonstrated.*

1 INTRODUCTION

The need for high–order accurate solvers are evident in applications where fine structures or wave propagation are of interest. Examples of such applications are aeroacoustics, turbulent flows and electromagnetics. The challenge when deriving a high-order accurate finite difference scheme is to obtain stability when boundaries are incorporated into the discrete operator. Often, the stability of the scheme is a too difficult task to investigate and hence one has to rely on the computational experience of the code. In a series of papers Nordström and Carpenter et al have used so called summation by parts (SBP) operators together with a weak imposition of the boundary and interface conditions via a penalty formulation to derive high–order accurate schemes that can be proved to be strictly stable for linear problems, [1], [4]–[8], [10], [11].

In this paper we evaluate the efficiency and stability of a high–order accurate multi-block parallel Navier-Stokes code, NS3D, on complex and time dependent flows. In NS3D, the SBP operators together with the penalty formulation have been implemented in three space dimensions. A particularly attractive feature of this multi-block technique is that no continuity requirements except matching gridlines are required at the interface.

As a test case the flow over a rectangular cavity in two dimensions was chosen. By altering the steepness and thickness of the boundary layer, respectively, at the leading edge of the cavity both shear layer mode and wake mode were obtained. The boundary layer was given at the leading edge of the cavity in contrast to other simulations where the data is normally given further upstream of the cavity. This rather crude approximation allows for a flexible simulation of different upstream environments.

The paper is organized as follows. In Sec 2 the numerical method and basic analysis is outlined. In Sec 3 details of the numerical code NS3D is presented. In Sec 4 we present the results of the numerical investigations for flow over a cavity in shear layer and wake mode, respectively. The focus is on the robustness and efficiency of the code. Finally in Sec 5 we make conclusions.

2 NUMERICAL METHOD

We briefly explain the numerical technique behind the code used in this paper, for more details see [1], [4]–[8], [10], [11]. As a model for the Navier-Stokes equations we consider the one-dimensional advection diffusion problem,

$$u_t + au_x = \epsilon u_{xx}, \quad 0 \leq x \leq 1, \quad t \geq 0, \quad a > 0, \quad \epsilon > 0, \tag{1}$$

augmented with initial condition and boundary conditions. The form of the boundary conditions that we consider is $au(0,t) - \epsilon u_x(0,t) = g_0(t), \quad -\epsilon u_x(0,t) = \epsilon g_1(t)$. In other words, we specify the total flux on the inflow boundary $x = 0$ and the viscous flux on the outflow boundary $x = 1$. That is essentially what is done in the code as well.

The energy method (we multiply with the solution and integrate over the domain) applied to (1) leads to,

$$||u||_t^2 + 2\epsilon||u_x||^2 = -a^{-1}\left[au(1,t) + \epsilon g_1(t)\right]^2 + \frac{(\epsilon g_1(t))^2}{a} - a^{-1}\left[au(0,t) - g_0(t)\right]^2 + \frac{g_0(t)^2}{a}. \tag{2}$$

A bounded energy clearly exist and the problem (1) is strongly well posed. Note that if $\epsilon \to 0$, the advection-diffusion equation, the boundary conditions and the estimate (2) goes smoothly over to a description of a well-posed advection problem (a model for the Euler equations).

2.1 The discrete problem

We use high order finite differences methods based on Summation-By-Parts (SBP) operators and penalty techniques for imposing the boundary conditions. A difference operator $D = P^{-1}Q$ approximating $\partial/\partial x$ is a first derivative SBP operator if $P = P^T > 0$ and $Q + Q^T = B = diag\,(-1, 0 \ldots, 0, 1)$. The semi-discrete approximation of (1) with the SAT penalty technique, see [1], for imposing the boundary conditions is

$$v_t + aDv = \epsilon D^2 v - P^{-1}\tau_0(E_0(aI + \epsilon D)v - e_0 g_0) - P^{-1}\tau_1(E_1(-\epsilon D)v - e_N \epsilon g_1). \quad (3)$$

The penalty parameters $\tau_{0,1}$ will be tuned to obtain stability. In (3) we have used $e_0 = (1, 0, \ldots, 0)^T, E_0 = diag(-1, 0 \ldots, 0, 1), e_N = (0, \ldots, 0, 1)^T, E_1 = diag(0, \ldots, 0, 1)$.

The energy method (multiply from the left with vP and use the SBP property $Q+Q^T = B$) applied to (3) yields

$$(||v||_P^2)_t + 2\epsilon||Dv||_P^2 = -a^{-1}\left[av_N + \epsilon g_1(t)\right]^2 + \frac{(\epsilon g_1(t))^2}{a} - a^{-1}\left[av_0 - g_0(t)\right]^2 + \frac{g_0(t)^2}{a}, \quad (4)$$

with the choice $\tau_0 = -1, \tau_1 = 1$. The estimate (4) is completely similar to (2) and the energy $||v||_P^2 = v^T P v$ is bounded. In fact, the approximation (3) is strongly stable.

One appealing character of the Navier-Stokes code NS3D is that it goes smoothly over to an Euler solver as the Reynolds number goes to infinity (or $\epsilon = 1/Re \to 0$). The way that this works can be seen in the following way. Let us rewrite the approximation (3) as (with $\tau_0 = -1$ and $\tau_1 = 1$ inserted)

$$v_t + aDv = -P^{-1}(E_0 av - e_0 g_0) + P^{-1}\epsilon([Q + E_0 - E_1]Dv + e_N g_1). \quad (5)$$

If $\epsilon \to 0$, the second penalty term in (5) vanish and we have an approximation of the advection problem. The corresponding energy estimate is obtained from (4) by simply letting $\epsilon = 0$.

Additional damping of arbitrary strength can be obtained by adding artificial dissipation operators of the form $DI_{2i}v = \nu P^{-1}\tilde{D}_i^T \Lambda \tilde{D}_i v$ to the righthand side of (3). The parameter ν has the appropriate sign and can be chosen to yield an upwind scheme. The operator $\tilde{D}_i$ is an undivided difference operators of order i and Λ is a diagonal matrix that is of order one in the interior of the domain an decreases smoothly to maintain the order of accuracy at the boundaries of the domain, see [4] for more details.

3 THE HIGH-ORDER ACCURATE NAVIER-STOKES CODE (NS3D)

The SBP operators together with penalty terms to impose the boundary conditions were implemented for the Navier–Stokes equations in three space dimensions. The numerical technique discussed above was used for the full three-dimensional code. The block interface procedure as well as the imposition of solid wall boundary conditions are also imposed in the same principal way. Note that the code is linearly stable (we can actually prove that, not only wish for it, see [12]) and that no technique that cannot be proven stable in a linear sense exist in the code.

The code can run with 2,4,6,8th order accuracy in the interior of the blocks. At boundaries and block interfaces the accuracy drops to 1,2,3,4th order which yields a global order of accuracy of 2,3,4,5th order, see [11]. The integration in time is performed using an explicit 5-stage low storage explicit Runge-Kutta scheme derived in [2]. No turbulence model was used.

4 NUMERICAL RESULTS

As a test case, two dimensional flow over a rectangular cavity was considered. The length to depth ratio (L/D) was 5. In all calculations the Mach number was set to M=0.5 and the Reynolds number based on the length of the cavity was $Re = 6000$. By varying the thickness of the boundary layer at the leading edge of the cavity, flows in shear layer and wake mode, respectively, were obtained. The boundary layer profile was given as boundary data at the leading edge of the cavity. In this way, the boundary layer was easily modified. This technique is unsuitable for detailed solutions of flows in wake mode, since in this case, the flow in the cavity interact with the boundary layer, see [9]. This effect is neglected when the boundary layer is prescribed at the leading edge of the cavity. As initial conditions we used free stream values in the domain above the cavity and zero flow with free stream states for the density and energy, respectively, inside the cavity. At the solid walls non-slip boundary conditions were used. At the outflow boundary free stream data was used together with free stream boundary conditions [12]. If not stated, the grid used was a 8 block grid with 129x129 grid points in each block, yielding a total number of grid points of about 133 000. The whole computational domain was $0 \leq x \leq 50$ and $0 \leq y \leq 10$. The grid was refined in the vicinity of the solid walls and stretched smoothly away from the walls. In all calculations the time step was $\Delta t = 1 \cdot 10^{-5}$. Unless otherwise stated, a fourth order accurate scheme was used in the inner of the domain together with a second order accurate scheme at the boundary, yielding a global accuracy of three.

4.1 Shear layer mode

With a boundary layer thickness $\delta = 0.078$ a flow in shear layer mode was obtain, see Figure 1 where the vorticity are shown in five snap shots of one period of the periodic motion. Detailed studies of the solution showed that very small errors were generated at the block interfaces also in regions of complex flows. Special attention was paid to the downstream upper corner of the cavity since three blocks meet at this grid point. It was found that the solutions behaved according to what can be estimated from theory also at this numerically difficult grid point. No problems with instabilities occurred during the runs.

We measured the pressure fluctuations on the downstream vertical wall inside the cavity and on the bottom of the cavity close to the downstream corner. The results are shown in Figure 2. From Figure 2 we estimated the Strouhal number $St = \frac{fL}{U}$ to $St = 0.8$. This is slightly above the Strouhal number of the second Rossiter mode for a M=0.5 flow which is approximately $St_2 \approx 0.75$, see [9].

A second simulation was performed using a sixth order internal scheme, together with

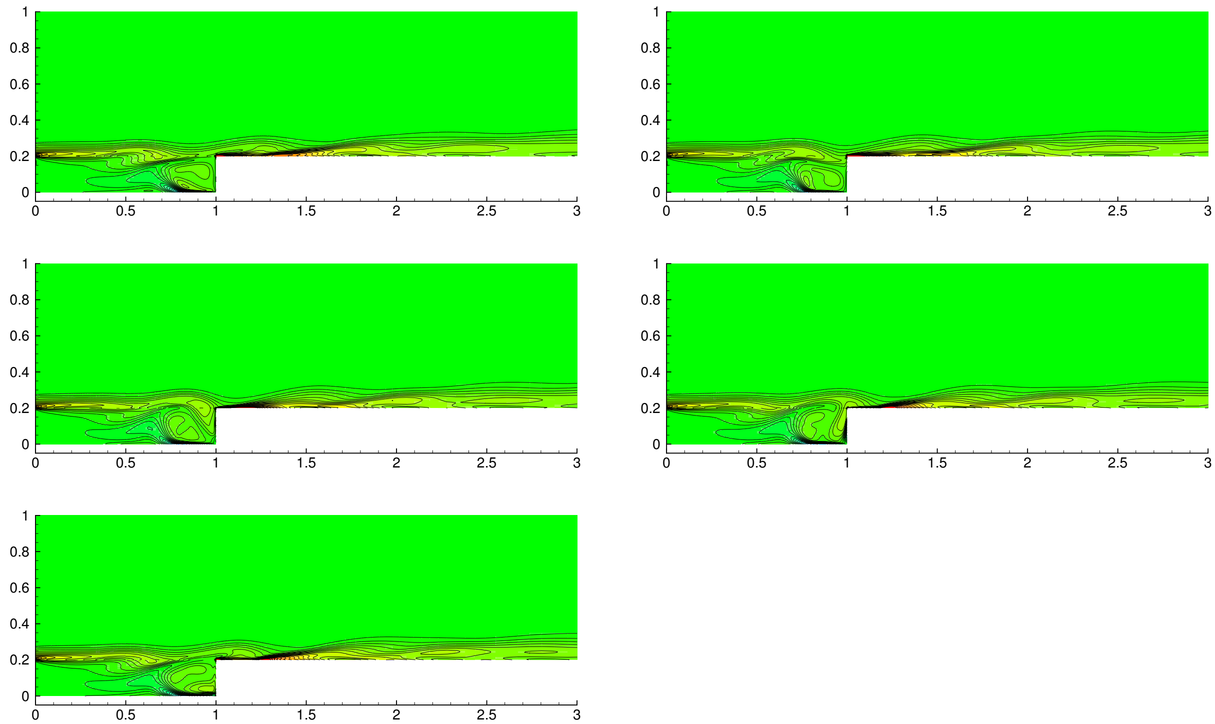

Figure 1: Contours of vorticity of flow in shear layer mode at $T = 33.5$, 34.0, 34.5, 35.0 and 35.5. $M = 0.5$, $Re = 6000$,$L/D = 5$.

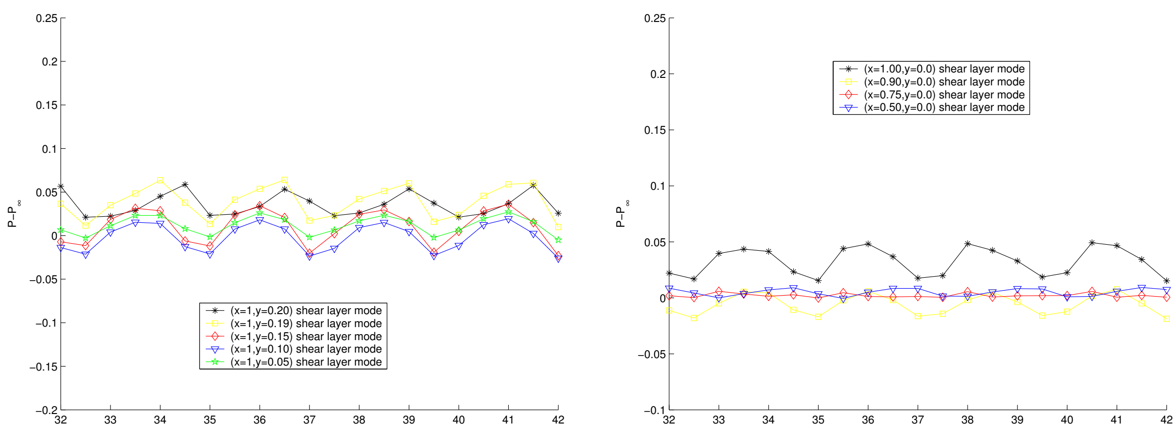

Figure 2: Pressure fluctuations on the wall inside the cavity. Shear layer mode $M = 0.5$, $Re = 6000$, $L/D = 5$. Left:Downstream vertical wall , y=0.20 (black), y=0.19 (yellow), y=0.15 (red), y=0.10 (blue) and y=0.05 (green), Right: Bottom wall , x=1 (black), x=0.9 (yellow), x=0.75 (red), x=0.5 (blue).

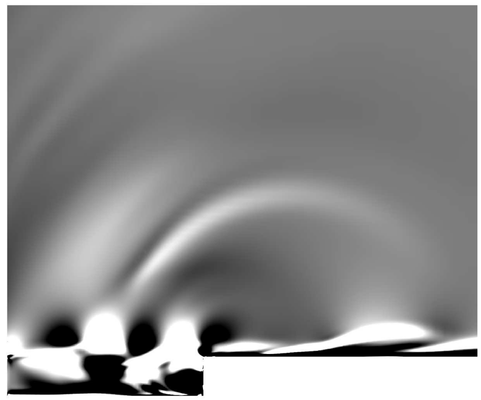

Figure 3: Contours of the density gradient $d\rho/dy$ of flow in shear layer mode.$M = 0.5$, $Re = 6000$, $L/D = 5$ A sixth order accurate scheme for the inner domain and a fourth order accurate scheme at the boundary has been used.

third order accuracy at the boundary. In this case the global order of accuracy is formally four. With this higher order accuracy the acoustic waves originating from the pressure fluctuations at the downstream side of the cavity were clearly seen, see Fig 3. These were not observed in the corresponding baseline calculation where a fourth order scheme was used for the inner domain and a second order accurate scheme at the boundary on the same computational grid.

4.2 Wake mode

By lowering the boundary layer thickness to $\delta = 0.0061$ at the leading edge of the cavity, a flow in wake mode was obtained. All other flow conditions and parameter settings were the same as for the shear layer mode simulations. This is in line with the results reported by Rowley et al, [9] where thinning of the boundary layer at the leading edge yielded a transfer from shear layer mode to wake mode. Four snap shots of the periodic solution are shown in Fig 4.2.

As for the shear layer mode case, no problems with stability were encountered during these more demanding simulations. The grid was stretched in the x-direction down-stream of the cavity, which damped the vortices that are ejected from the cavity.

We measured the pressure fluctuations at the downstream vertical wall inside the cavity and on the bottom of the cavity close to the downstream corner. The results are shown in Figure 5. The dominating frequency is lower compared to frequency of the shear layer

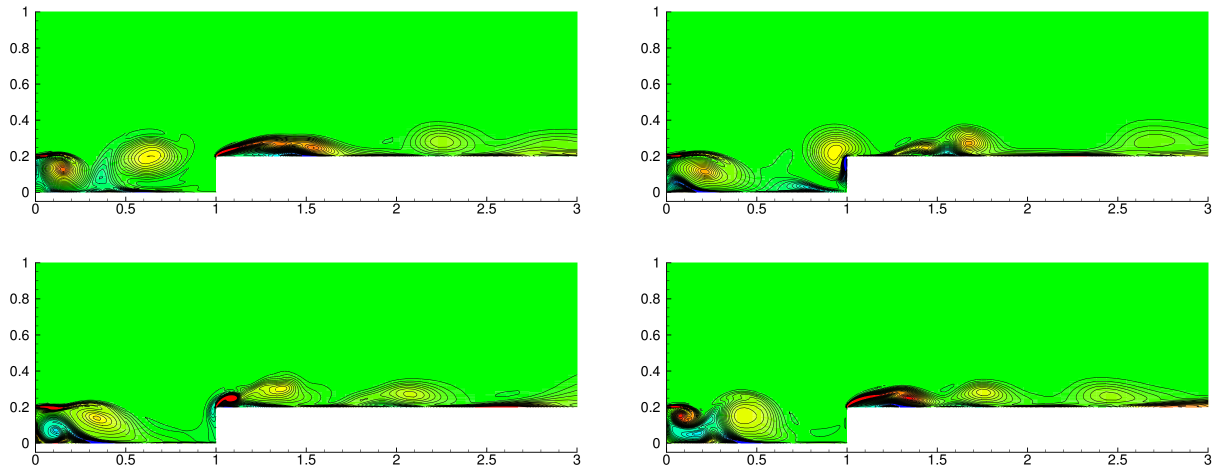

Figure 4: Contours of vorticity of flow in wake mode at $T = 32.5$, 34.0, 35.5 and 37.0. $M = 0.5$, $Re = 6000$, $L/D = 5$.

mode. From the picture we estimated the Strouhal number to be $St = 0.3$. This is in good agreement with the first Rossiter mode with an approximate Strouhal number of $St_1 \approx 0.3$, [9]. This is also reported in [9].

As a test, we raised the Reynolds number to $Re = 10^6$. This complies that the influence of the viscous terms are lowered (almost neglected) also in the boundary conditions. As can be seen in Eq (5), as the Reynolds number is increased (or equivalently ϵ decreases) but keeping the grid fixed, the boundary conditions will approach the Euler boundary conditions at a wall. Hence, the solution for a high Reynolds number without a turbulence model, will in principle be a solution to the Euler equations. However, the influence of the boundary layer thickness at the leading edge will still be inherent, since the boundary layer is given by boundary data. Note that the same boundary conditions as for the well-resolved base line test case with $Re = 6000$ was used in this calculation. As in the simulations presented above, no problems with numerical instabilities occurred during the calculations with $Re = 10^6$.

4.3 Efficiency and robustness

The numerical schemes used are very well suited for parallel calculations and the code NS3D has been parallelized using MPI. All calculations presented in this paper were performed using 8 processors. The scalability of a 2D code using the same numerical schemes as in the present 3D version has been investigated previously. See [3], in which an almost linear scalability is reported.

The code has proven to be extremely stable, even though complex non-linear flow fields have been studied. We performed simulations of the base line test case in both shear layer mode and wake mode using a computational grid with jumps in the grid cell sizes at the

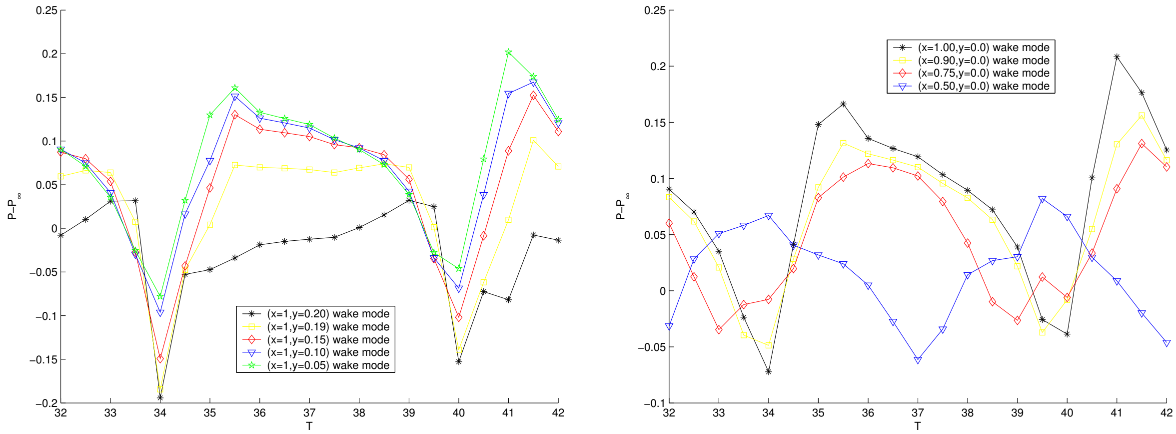

Figure 5: Pressure fluctuations on the wall inside the cavity. Wake mode $M = 0.5$, $Re = 6000$, $L/D = 5$. Left:Downstream vertical wall , y=0.20 (black), y=0.19 (yellow), y=0.15 (red), y=0.10 (blue) and y=0.05 (green), Right: Bottom wall , x=1 (black), x=0.9 (yellow), x=0.75 (red), x=0.5 (blue).

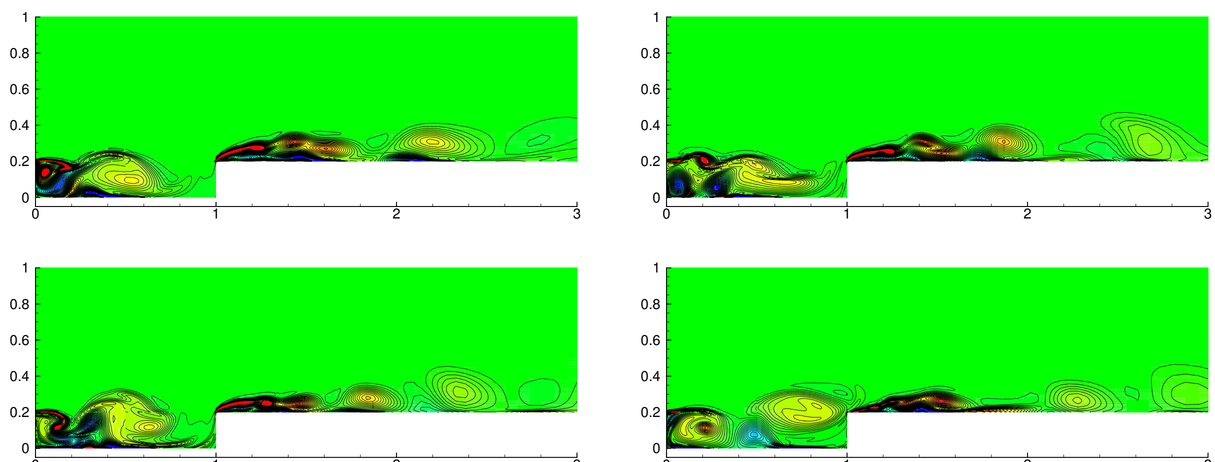

Figure 6: Contours of vorticity of flow in wake mode at $T = 32.5$, 34.0, 35.5 and 37.0. $M = 0.5$, $Re = 10^6$, $L/D = 5$.

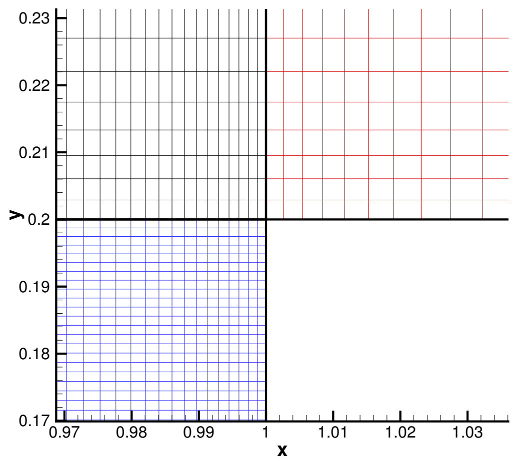

Figure 7: Computational mesh with jumps in the grid cell sizes at the interfaces. Blow up at the downstream upper corner of the cavity

interfaces, see Fig 7. The results were very close to those using matching grid cell sizes at the interfaces. No problems with instabilities occurred.

Another feature demonstrating the robustness of the code is its ability to handle the inflow boundary data used in these above mentioned test cases. Not shown here, we have also performed simulations with a boundary layer of zero thickness given at the inflow, that is, free stream data were given all the way down to the wall of the upper upstream corner of the cavity. Although unphysical, no problems with numerical instabilities were experienced.

5 CONCLUSIONS

We have evaluated the performance of a high-order accurate Navier-Stokes code for simulation of complex time-dependent flows in two space dimensions. The numerical method, which can be proved to be linearly stable, have shown to be extremely stable also for non-linear flow cases. The two dimensional flow over a cavity has been investigated for flows in both shear layer mode and wake mode, respectively. Flows in the two different modes were obtained by varying the boundary layer thickness at the upstream upper corner of the cavity. This technique, although physically doubtful for flow in wake mode, proved very efficient in the calculations and demonstrated in a clear way the robustness of the code. We also tested the robustness by using a grid with non-matching grid cell sizes at the block interfaces. The simulations were performed using the same parameter setup as for a grid with matching grid cell sizes and no problems with instabilities were obtained.

When raising the order of the accuracy acoustic waves that are originating from the pressure fluctuations at the downstream vertical wall of the cavity were seen.

All simulations showed good qualitative agreement with the results presented in [9]. In this paper, however, we have used a coarser grid and further investigations have to be performed in order to compare the results quantitatively.

REFERENCES

[1] M. H. Carpenter, J. Nordström and D. Gottlieb, A *Stable and Conservative Interface Treatment of Arbitrary Spatial Accuracy*, Journal of Computational Physics, Vol 148 No. 2, pp. 341-365, 1999.

[2] C.A. Kennedy, M.H. Carpenter and R. M. Lewis, *Low-storage, explicit, Runge-Kutta schemes for the compressible Navier-Stokes equations*, Applied Numerical Mathematics, Vol. 35, 2000.

[3] K. Mattsson M. Svärd, M. Carpenter, and J. Norström, *Accuracy Requirements for Transient Aerodynamics*, AIAA paper 2003–3689, 16th AIAA Compuational Fluid Dynamics Conference, Orlando, Florida.

[4] K. Mattsson M. Svärd and J. Nordström, *Stable and Accurate Artificial Dissipation*, Journal of Scientific Computing, Volume 21, No. 1, pp. 57-79, 2004.

[5] K. Mattson and J. Nordström, *Finite Difference Approximations of Second Derivatives on Summation by Parts Form*, Journal of Computational Physics, Vol. 199, pp. 503-540, 2004.

[6] J. Nordström and M. H. Carpenter, *Boundary and Interface Conditions for High Order Finite Difference Methods Applied to the Euler and Navier Stokes Equations*, Journal of Computational Physics, Vol 148 No. 2, pp. 621-645, 1999.

[7] J. Nordström and M. H. Carpenter, *High Order Finite Difference Methods, Multidimensional Linear Problems and Curvilinear Coordintes*, Journal of Computational Physics, Vol 173, pp. 149-174, 2001.

[8] J. Nordström and R. Gustafsson, *High Order Finite Difference Approximations of Electromagnetic Wave Propagation Close to Material Discontinuities*, Journal of Scientific Computing, Vol 18, No 2, 2003.

[9] C. W. Rowley, T. Colonius and A. J. Basu, *On Self-sustained Oscillations in Two-Dimensional Compressible Flow over Rectangular Cavities*, J Fluid Mech, vol 455, pp 315–346, 2002.

[10] M. Svärd, K. Mattsson and J. Nordström, *Steady State Computations Using Summation-By-Parts Operators*, Journal of Scientific Computing, Volume 24, No. 1, pp. 79-95, 2005.

[11] M. Svärd and J. Nordström, *On the Order of Accuracy for Difference Approximations of Initial-Boundary Value Problems*. In press in Journal of Computational Physics.

[12] M. Svärd, M.H. Carpenter and J. Nordström, *A stable high-order finite difference scheme for the compressible Navier-Stokes equations*, in preparation.

[13] O.C. Zienkiewicz and R.L. Taylor. *The finite element method*, McGraw Hill, Vol. I., (1989), Vol. II., (1991).

[14] S. Idelsohn and E. Oñate. Finite element and finite volumes. Two good friends. *Int. J. Num. Meth. Engng.*, **37**, 3323–3341, (1994).